# Elemental diffusion chronostratigraphy: time-integrated insights into the dynamics of plumbing systems

Chiara Maria Petrone[1] and Martin Mangler[1]

[1]The Natural History Museum

November 24, 2022

**Abstract**

Time-related information of pre-eruptive magmatic processes is locked in the chemical profile of compositionally zoned minerals and can be retrieved by means of elemental diffusion chronometry. However, only the timescale of the outermost rim is commonly resolved, limiting our knowledge of timescales to those directly preceding the eruption. A major obstacle is the need to accurately constrain temperatures at which diffusion occurred. This is particular difficult for multiple zoned minerals where the different compositional boundaries indicate multiple physicochemical changes of melt environments during the lifetime of a crystal. Here, we argue that elemental diffusion chronostratigraphy can be fully resolved for crystals that have spent their lifetime in hot storage. Under this condition, crystals will be kept at the temperature of the eruptible magma(s), and diffusion timescales approximate the storage of the crystal in question in different melt environments. We further argue that hot storage conditions are typical of open-conduit systems in steady-state and are driven by the regular supply of fresh hot magmas determining the constant presence of eruptible magma. Fe-Mg interdiffusion in pyroxenes from Stromboli and Popocatepetl volcanoes are used as examples to reconstruct the time-dependent elemental diffusion chronostratigraphy of single crystals and discuss magma dynamics implications. Uncertainties introduced by temperature estimates and other input data, including experimentally derived values for the activation energy E and the pre-exponential factor D0, have large effects on the accuracy of modelled timescales, which need to be correctly evaluated and mitigated. Elemental diffusion chronostratigraphy is an extremely powerful tool to obtain time-related temporal information on the dynamics and histories of volcanic plumbing systems, which can lead to an in-depth knowledge of the magmatic system far beyond late-stage pre-eruptive processes. Combined with monitoring data and other petrological, geological and geophysical constraints at active volcanoes, they can greatly enhance our capability to inform volcanic hazard assessments.

AGU Monograph on Crustal Magmatic System Evolution: Anatomy, Architecture, and Physico-Chemical Processes - Section iii – 13. Diffusion timescales in igneous systems

# Elemental diffusion chronostratigraphy: time-integrated insights into the dynamics of plumbing systems

C.M. Petrone*, M.F. Mangler

The Natural History Museum, Department of Earth Sciences, Cromwell Road,

SW7 5BD, London, United Kingdom, *corresponding author: c.petrone@nhm.ac.uk

## Abstract

Time-related information of pre-eruptive magmatic processes is locked in the chemical profile of compositionally zoned minerals and can be retrieved by means of elemental diffusion chronometry. However, only the timescale of the outermost rim is commonly resolved, limiting our knowledge of timescales to those directly preceding the eruption. A major obstacle is the need to accurately constrain temperatures at which diffusion occurred. This is particular difficult for multiple zoned minerals where the different compositional boundaries indicate multiple physicochemical changes of melt environments during the lifetime of a crystal.

Here, we argue that elemental diffusion chronostratigraphy can be fully resolved for crystals that have spent their lifetime in hot storage. Under this condition, crystals will be kept at the temperature of the eruptible magma(s), and diffusion timescales approximate the storage of the crystal in question in different melt environments. We further argue that hot storage conditions are typical of open-conduit systems in steady-state and are driven by the regular supply of fresh hot magmas determining the constant presence of eruptible magma.

Fe-Mg interdiffusion in pyroxenes from Stromboli and Popocatépetl volcanoes are used as examples to reconstruct the time-dependent elemental diffusion chronostratigraphy of single crystals and discuss magma dynamics implications. Uncertainties introduced by temperature estimates and other input data, including experimentally derived values for the activation energy $E$ and the pre-exponential factor $D_0$, have large effects on the accuracy of modelled timescales, which need to be correctly evaluated and mitigated.

Elemental diffusion chronostratigraphy is an extremely powerful tool to obtain time-related temporal information on the dynamics and histories of volcanic plumbing systems, which can lead to an in-depth knowledge of the magmatic system far beyond late-stage pre-eruptive processes. Combined with monitoring data and other petrological, geological and geophysical constraints at active volcanoes, they can greatly enhance our capability to inform volcanic hazard assessments.

**Keywords:** Elemental diffusion, Geospeedometry, Timescales, Residence time, Hot storage, Steady-state

**Running title:** Diffusion Chronostratigraphy

## Introduction

It has long been known that minerals preserve information about the environment they grew in, representing a valuable archive of geological information (e.g., Streck, 2008, Cooper, 2017). In the case of igneous minerals, crystallized from a magma, a range of information regarding pre-eruptive or pre-emplacement processes are locked in the mineral's compositional profile. Pressure and temperature of crystallization can be unlocked via the usage of barometers and thermometers (e.g., Putirka, 2008). Compositional zoning is commonly linked to magma mixing processes, although they also reflect variations in physical conditions (e.g., P, T, $fO_2$ and $H_2O$), particularly but not exclusively in plagioclase (e.g., Anderson, 1984; Streck, 2008; Giacomoni et al., 2014). Isotope variability from different portions of the crystal can reveal crustal contamination alongside magma mixing processes (e.g., Davidson et al., 2007). Minerals can also provide time-related information. Radiometric dating techniques have long been used to provide absolute ages of minerals' crystallization (e.g, Cooper, 2019 and reference therein), whereas diffusive timescales provide constraints on the time crystals might have spent in crustal magma reservoirs relative to pre-eruption processes (e.g., Zellmer et al.,1999; Mangler et al., 2020). In the last decade, following pioneering studies of timescales of metamorphic processes (e.g., O'Brien & Vrána, 1995; Ganguly et al., 1996; Ayers & Vance, 1997), elemental diffusion modelling has proved an invaluable instrument to infer timescales of pre-eruptive magmatic processes, such as the timing of magma injections into shallow reservoirs, magma mush remobilization, and ascent rate (e.g., Turner & Costa, 2007; Costa et al., 2008; Petrone et al., 2016, 2018; Dohmen et al., 2017).

The radiometric clock starts at temperatures below the closure temperature of the relative radiometric system, which in most cases corresponds to the age of the crystal growth (i.e., absolute crystallization age) constraining the longevity of a magmatic system (Cooper, 2019 and references therein). The diffusive chronometer starts upon the formation of a chemical gradient. Temperature is strongly controlling the rate of the diffusive smoothing of the chemical gradient even after the compositional boundary has been isolated from the melt (i.e., overgrowth of a further external crystal's portion). On the contrary, the radiometric clock is insensitive to changes in temperatures subsequent to crystal growth, unless the temperature rises above the closure temperature where the radiometric clock will reset. Radiometric ages are a mixed record from different portion of crystals (i.e., old cores and rims) spanning a large range ($10^4$-$10^5$ years) and providing average absolute crystallization ages, which in most cases are unaffected by diffusion, due to the very slow diffusion rate of the elements in question (e.g., U series, Cooper & Kent, 2014). Elemental diffusion timescales usually record much shorter

timescales (hours to $10^3$ years, e.g., Cooper & Kent, 2014; Cooper, 2019 and references therein), which are commonly interpreted to represent late-stage, short-lived processes such as final magma mixing and assembly before an eruption. This is due to the intrinsic nature of elemental diffusion processes that requires the presence of a compositional gradient, therefore the history of an unzoned crystal (or the unzoned portion of a zoned mineral such as the crystal's core) cannot be determined via geospeedometry.

The majority of elemental diffusion models focus on the outermost rim of crystals yielding time constraints only on the final stage of the crystal's history (e.g., see Costa et al., 2008; Dohmen et al., 2017 and Cooper, 2019 for a review). Recently, however, several authors have attempted to resolve more than one compositional boundary to approach a comprehensive crystal chronostratigraphy (Kahl et al., 2011; Druitt et al., 2012; Petrone et al., 2016; 2018; Rout et al., 2020). When the elemental diffusion profile can be resolved for several compositional boundaries in the same crystal, a closer correspondence between diffusion timescales and radiometric ages tracking the same event can be expected. This allows a more in-depth reconstruction of the dynamics of the plumbing system, alongside a time-constrained sequence of magmatic processes. This information is fundamental in case of active volcanoes and can be used in combination with monitoring data and other geological, seismic and petrological constraints to assess volcanic hazard.

The overall goal of this paper is to explore the potential of geospeedometry to resolve time-integrated information stored in the stratigraphy of zoned crystals beyond the final pre-eruptive stages, and to highlight pitfalls related to the approach. We will present examples from Stromboli and Popocatépetl volcanoes, using the recently published non-isothermal step diffusion model (NIDIS, Petrone et al., 2016) as one example of the many possible approaches to resolve single crystal elemental diffusion chronostratigraphy, with the aim to contribute toward a better understanding of magmatic system dynamics.

## Geospeedometry: approach and limitations

The possibility of extracting the time elapsed between a magma mixing event and eruption is based on two main assumptions: change of thermodynamic equilibria during the mixing process, leading to the formation of a compositional boundary within a crystal and subsequent elemental diffusion at the boundary; and an elemental diffusion rate close to zero upon eruption. The first assumption is a consequence of the mixing process between two magmas characterised by different physical (i.e., T, $fO_2$) and chemical composition (including gas and crystal contents) leading to the formation of compositionally zoned crystals. An implicit corollary of this assumption is that the crystal will experience instantaneous growth upon mixing, which might be preceded by dissolution. Normally crystal growth rates are orders of magnitude higher than elemental diffusion rates, even for relatively fast diffusing elements such as Fe-Mg in pyroxenes (e.g., Dimanov & Sautter, 2000; Ni et al., 2014).

Therefore, in many cases, it is safe to assume an instantaneous crystal growth (e.g., Costa et al., 2008; Petrone et al., 2016).

Elemental diffusion is a time (*t*)- and temperature (T)-dependent process (e.g., Crank, 1975), with the diffusion rate increasing with increasing T. The effect of intra-crystal elemental diffusion is to smooth the initial sharp compositional profile at the boundary between two different portions of a compositionally zoned crystal. The diffusive relaxation of the compositional profile is a function of the time spent at magmatic temperature and the rate of diffusion, which is mineral specific and further controlled by temperature, oxygen fugacity and crystallographic direction (in anisotropic minerals). Upon eruption the low (i.e., atmospheric) T will drive the diffusion rate for most elements and minerals effectively close to zero, freezing the diffusion profile and therefore preserving the time spent at the high T of the magmatic environment (e.g., Costa et al., 2008; Dohmen et al., 2017). This can be retrieved by means of elemental diffusion modelling. The extent of diffusion in minerals (i.e., the distance affected by diffusion) is a function of the square root of the time (*t*) over which the diffusion acted and the diffusion coefficient D ($x \cong \sqrt{tD}$ eq. 9, Zhang, 2010). It is therefore clear that in order to calculate the time *t* related to a diffusion profile, the diffusion coefficient must be known. The diffusion coefficient is a function of T as expressed by the Arrhenius relationship:

$$D = D_0 e^{-E/RT} \qquad (1)$$

where $D_0$ is the pre-exponential factor, E the activation energy, R the gas constant and T the absolute temperature in K. The dependence of D on T means that in order to resolve the diffusion equation and calculate the time *t*, the temperature at the time of diffusion must also be known. In addition, the exponential relationship means that any error on T can affect the uncertainty on the timescales by orders of magnitude (i.e., from 40% to 20% on clinopyroxene when the error on T decrease from ±15°C to ±6°C, Petrone et al., 2016; Scarlato et al., this issue). T and D are the main parameters controlling elemental diffusion in minerals and we shall explore in detail the uncertainties introduced by these parameters in a separate section.

There are many excellent publications about the theoretical framework of diffusion modelling, with published analytical and numerical solutions of the diffusion equations (e.g., Crank, 1975; Chakraborty, 2006, Costa et al., 2008, Zhang, 2010, Petrone et al., 2016, Dohmen et al., 2017). It is not the scope of this paper to repeat those works, but it is important to highlight some of the caveats and assumptions inherent to diffusion models, before exploring in detail challenges and opportunities offered by resolving crystals' elemental diffusion stratigraphy.

Initial and boundary conditions must be inferred or established before modelling the diffusion profile. The initial zoning profile can be assumed as gradual, abrupt, homogenous or oscillatory (Costa et al., 2008) reflecting different magmatic processes and minerals. A common approach for pyroxene is to use slow-diffusing elements to infer the initial profile of fast diffusing elements (e.g., Costa et al.,

2008, Allan et al., 2013, Petrone et al., 2016). For plagioclase an initial step function profile is assumed and the fast diffusing profile of Sr and Mg is inferred from the slow diffusing profile of CaAl-NaAl (e.g., Costa et al., 2003,Costa et al., 2008; Dohmen et al., 2017). For olivine the initial profile is considered unzoned (e.g., Costa et al., 2008; Kahl et al., 2011). In the case of sanidine, provided that Sr distribution mimics Ba, the diffusion of Ba is compared with Sr diffusion modelling to ensure modelling of true diffusive profiles (Chamberlain et al., 2014).

The nature of exchange between the crystal and its surrounding matrix determines the nature of the boundary conditions, which can be open or closed (e.g., Crank, 1975; Chakraborty & Ganguly, 1991; Costa et al., 2008; Mueller et al., 2010). Open boundaries are far more common in magmatic systems than closed boundaries characterized by no diffusive flux of the element of interest in and out of the crystal (i.e., the elements of interest do not significantly partition in the surrounding phase or the diffusion rate in the matrix is much slower than in the mineral, Costa et al., 2008). In the case of open boundaries there is diffusive communication between the two sides, but depending on the conditions it can result in a variable concentration (e.g., the melt reservoir has limited volume or the ambient conditions change significantly) or fixed concentration (e.g., assuming a diffusive exchange with a large volume of melt). Accordingly, the initial conditions are assumed equal to the maximum and minimum compositions (using concentration plateaux when possible) and the diffusion profile will ultimately equilibrate within the mineral homogenizing at an intermediate level (i.e., finite reservoir of limited extent). On the contrary, in case of infinite reservoirs (i.e., the condition mostly characterising rims) the element concentration will also depend on the partition coefficient between mineral and melt, which will control the final concentration that is fixed at the crystal rim (Mueller et al., 2010). In cases when the initial profile cannot be easily inferred, due to the lack of a clear plateau, an arbitrary maximum value, corresponding to a step function based on the range of natural compositional variation, can be assumed (Zellmer et al., 1999, Petrone et al., 2016).

Non-cubic minerals are anisotropic in terms of elemental diffusion rates, in the same way as their optical properties. This is particularly important for olivine where elemental diffusion along the *c*-axis is six times faster than along the *a*- and *b*-axes (Tachibana et al., 2013, Dohmen et al., 2017). It is therefore critical to the accuracy of timescales calculated from diffusion models, to precisely identify the crystallographic direction along which the diffusion profile is modelled. This can be satisfactorily approximated for pyroxene and plagioclase on the basis of their optical characteristics. For example, Fe-Mg diffusion profiles have been measured perpendicular to the (100) plane in recent works on pyroxene (Morgan et al., 2006; Petrone et al., 2016; 2018), which can be identified to a certain degree of accuracy under an optical microscope. In other cases where the optical properties cannot help to identify the crystallographic direction, or when there is a need of very precise and accurate information on crystal's orientation as for example in olivine, electron back-scattered diffraction (EBSD) is used to determine the exact crystallographic direction and the diffusion profile is calculated

accordingly to trigonometric rules (Costa et al., 2008; Kahl et al., 2011; Dohmen et al., 2017). A further complication arises from sectioning effects due to the fact that most diffusion models are done in 1-D space based on a random 2-D thin section of a crystal, with no information on the actual 3-D geometry. For example, it is not necessarily possible to infer from a given crystal section whether it cuts through the crystal core or if it is off-centred. Neglecting the effect of 2-D and 3-D geometry results in a significant mismatch of the modelled timescales (Costa et al., 2003; 2008, Shea et al., 2015; Krimer & Costa, 2017). Some strategies to mitigate this effect such as measuring the diffusion profile along the *b*-axis for pyroxene, using symmetrical profiles (Krimer and Costa, 2017), comparing 1-D model with ideal 3-D numerical model (Shea et al., 2015) have been proposed, but the problem is yet to be fully resolved.

**Isothermal *vs.* non-isothermal approach**

Magmatic processes are non-isothermal. Magmas crystallize over a range of temperatures and the temperature contrast during magma mixing can be as high as 300ºC (e.g., Hawkesworth et al., 2000, Kent et al., 2010). Constraining the range of temperatures from a minerals' compositional profile is not a straightforward task. Pre-eruptive temperatures can be calculated using different types of geothermometers, if an equilibrium between mineral and melt or between two coexisting mineral phases can be demonstrated (e.g., Putirka, 2008). A single pre-eruptive temperature, obtained from equilibrium between the crystal's rim and the matrix, is commonly assumed to calculate timescales of pre-eruptive processes (e.g., Costa et al., 2003; Morgan et al., 2004; Allan et al., 2013, Kilgour et al., 2013). However, this temperature in many cases reflects the latest magmatic environment experienced by the crystal prior to the eruption, but it cannot accurately reflect the entire thermal history of the crystal. In fact, as crystals grow from core to rim, their composition changes as a function of temperature and other physicochemical parameters as they move through different magmatic environments. Furthermore, widespread disequilibrium between melt and minerals (e.g., Couch et al., 2001; Spark & Cashman, 2017) in many volcanic products worldwide indicate that calculated temperatures do not represent the entire magma reservoir during pre-eruptive magma assembly (e.g., Coper & Kent, 2014). Crystals may not only experience multiple magmatic environments during their lifetime (e.g., antecryst, different portion of zoned crystals; e.g., Fabbro et al., 2013; Kahl et al., 2013; Mangler et al., 2020), but they also spend variable time (i.e., storage) in each environment. This often results in complex zoning patterns reflecting the crystal's history of growth, mixing and storage in different magmatic environments, at often dramatically different temperatures (e.g., Cooper, 2017; 2019; Petrone et al., 2018; Di Stefano et al., 2020).

In the attempt of resolving with greater accuracy the lifetime history of crystals from their core-to-rim compositional diffusion profile, increasing attention has been devoted to characterize the different

melt environments, moving from an isothermal to a non-isothermal approach. A system analysis approach has been used to reconstruct compositional zoning patterns in olivines derived from different magmatic environments (Kahl et al., 2011). However, only the time spent in the final pre-eruptive magmatic environment has been modelled for most of the olivines (e.g., Kahl et al., 2011; 2013). Using a forward approach with a two-step diffusion model, Druitt et al. (2012) modelled the core-rim diffusion profile of plagioclase from Santorini volcano assuming equilibrium with two melts of differing compositions and temperatures. More recently, a non-isothermal approach to elemental diffusion (i.e, NIDIS, Petrone et al., 2016) has been proposed to resolve complex core-rim elemental diffusion profiles of clinopyroxene from Stromboli volcano (Petrone et al., 2016; 2018). Working inwards from crystal rim to core, the elemental diffusion stratigraphy profile is deconstructed in single isothermal steps, each one characterized by a specific temperature and diffusion coefficient reflecting the change in magmatic environment, providing the timescales spent in each of those environments. This approach has resulted in a better understanding of the timescales and dynamics of magma mixing, storage, and eruption-trigger events in a steady-state magmatic system (i.e, constant rate of input and output; Petrone et al., 2018). Recently, the NIDIS model was experimentally validated by Rout et al. (2020), who further presented a simplified, mathematically equivalent algorithm yielding reduced propagated errors and therefore improved precision of diffusion timescales.

**The temperature conundrum**

A critical aspect of any elemental diffusion study is the availability of the actual diffusion temperatures at which crystals are stored before eruption. Recently, some authors suggested that magmatic systems spend most of their life in cold storage as almost solid crystal mush, with short and ephemeral bursts of high temperature during remobilization of the mush by mafic magmas, eventually triggering the eruption (e.g., Cooper & Kent, 2014; Cashman & Giordano, 2014). The implication is that the temperature(s) at which crystals spend most of their time is significantly lower than that of the melt from which the crystals grew in and might be difficult to constrain via thermometry (Cooper & Kent, 2014). Therefore, crystal storage times will be much longer than the diffusive timescales modelled from diffusion between magma remobilization and eruption (i.e., the ephemeral hot burst). If the temperature of the cold-storage cannot be calculated, then it would be impossible to estimate the time the crystal spent in the cold storage. In this case, diffusive timescales will only represent the final portion of the story and determining the timescales of multiple events of crystal-rich melt movements between different magmatic environments might be difficult.

However, we argue that if the system is kept at hot storage conditions, which implies the presence of eruptible magma (i.e., <40% crystals, Burgisser & Bergantz, 2011) at temperatures well above the locked crystal mush, crystals will spend their lifetime at the temperature of the eruptible magma in the corresponding magmatic environment. Under this condition, diffusive timescales (from models at the

temperatures of the eruptible melt) approximate the storage of the crystals in question (Petrone et al., 2018). Hot storage might be a common condition in open-conduit systems with a frequent input of recharging mafic magma. Hot storage with a continual presence of melt has been suggested for the Soufrière Volcanic Centre (Santa Lucia, Barboni et al., 2016), Popocatépetl (Mangler et al., 2020), and Laacher See volcano (Rout & Wörner, 2020), and might therefore be a common condition in arc volcanoes. Recent work on Stromboli volcano has shown agreement between clinopyroxene elemental diffusion timescales and U-Th residence times calculated for the 2-4 km shallow reservoir of Stromboli (Petrone et al., 2018), suggesting that they are both tracking the residence time at magmatic temperatures of the shallow reservoir, where mixing processes between resident magma, incoming magma and the mush occur. Considering that according to Bragagni et al. (2014), the mush is constituted by a solid portion (i.e., antecrysts) and by an interstitial liquid (i.e., *antemelt*), and that the *antemelt* actively contributes to the magma mixing process upon remobilization by the incoming more mafic and hotter magma, we can infer that the mush must be kept at temperatures well above the near-solidus condition for prolonged time. Therefore, in magmatic systems characterized by hot storage conditions, the storage time of the chemically zoned portion of the crystal can be approximated by the total diffusive timescales occurring at the temperatures of the relative melt environments producing the compositional banding.

On this basis, we argue that hot storage is common for steady-state open-conduit systems, which are often also characterised by a limited whole rock compositional variation over a protracted length of time (e.g., basaltic composition at Stromboli and Etna, Francalanci et al., 1999; Di Renzo et al., 2019; andesitic-dacitic at Popocatépetl, Mangler et al., 2019). Open-conduit conditions associated with a buffered compositional range, which can last several thousands of years (Mangler et al., 2019), indicate that such magmatic systems are controlled by processes constant over a long period of time, and magma hybridization between long-lived end-members is the most probable process (e.g., Petrone et al., 2018; Di Renzo et al., 2019; Mangler et al., 2019; 2020).

If storage time and elemental diffusion timescales can be equated in steady-state open conduit volcanoes, and if the various magmatic environments (i.e, magma end-members and related hybrid compositions) can be fully characterised using mineral-melt and mineral-mineral geothermometers, then these temperatures can be used to calculate diffusion timescales in each magmatic environment, and to fully reconstruct the crystallisation and storage history of individual crystals (Kahl et al., 2011; Petrone et al., 2016; 2018). In the case of Stromboli, where the two end-members have been recognized and fully characterized (e.g., Francalanci et al., 1999; De Carlo et al., 2006; Pichavant et al., 2009; Bragagni et al., 2014), temperatures have been estimated using a combination of experimental data (De Carlo et al., 2006; Pichavant et al., 2009), clinopyroxene-liquid thermometers and MELTS simulations (Petrone et al., 2018). At Popocatèpetl the equilibrium between ortho- and

clinopyroxene, over their entire compositional range, has been used to estimate the magmatic temperature corresponding to each portion of a zoned pyroxene (Mangler et al., 2020).

**Two examples: Stromboli and Popocatépetl volcanoes**

Elemental diffusion stratigraphy has previously been resolved, using the NIDIS approach, for Fe-Mg interdiffusion in clinopyroxene of Stromboli with variously complex compositional zoning (Petrone et al., 2016; 2018). Here we revisit the main findings of those studies and present some further examples of pyroxenes from Popocatépetl volcano.

Stromboli stratovolcano in the Aeolian Islands (Southern Italy) is one of the best studied volcanoes worldwide. Continuous and moderately explosive 'Strombolian' activity characterises at least the last 2,000 years. The typical Strombolian activity is accompanied by periodic lava flows and interposed with more violent eruptions (paroxysm) tapping a deeper reservoir (e.g., Bertagnini et al., 2008; Francalanci et al., 2013). Stromboli has long been recognised as a typical steady-state volcano, with a shallow magmatic reservoir (highly porphyritic or *hp*-magma) refilled continuously and at constant rate by more mafic deeper magma (low porphyritic or *lp*-magma) and accompanied by mixing, crystallisation and eruption (e.g., Francalanci et al., 1999; Bragagni et al., 2014).

Popocatépetl stratovolcano is located in central Mexico and is characterised by a wide variety in eruptive styles typical for subduction zone volcanism. Present-day activity initiated in December 1994 and is characterised by dome-building and -destruction cycles associated with mild to moderate Vulcanian eruptions (Gómez-Vazquez et al., 2016). Past activity included at least six Plinian eruptions in the last ~23.5 ka (Schaaf et al., 2005; Arana-Salinas et al., 2010; Sosa-Ceballos et al., 2014; Siebe et al., 2017) and interplinian emplacement of several voluminous lava flows (Mangler et al., 2019). Popocatépetl lavas and pumices are calc-alkaline andesites and dacites that underwent varying degrees of lower and upper crustal assimilation *en route* to the surface (Schaaf et al., 2005; Sosa-Ceballos et al., 2014; Mangler et al., 2019). Frequent mixing and hybridisation of geochemically distinct magmas effectively buffers whole rock compositions favouring the eruption of a narrow compositional range in the last ~23.5 ka (Mangler et al., 2019; 2020).

We will discuss the general implications for the dynamics of an open-conduit plumbing system arising from the presented examples to illustrate the potential of elemental diffusion chronostratigraphy, however it is not the scope of this work to discuss in any detail the specific implications either for Stromboli or for Popocatépetl. It is important to stress that in order to fully understand the dynamics of a specific volcanic system, the crystal cargo needs to be examined and characterized in detail. Such work is fundamental to geospeedometry, since different populations of a mineral phase might represent different magmatic processes and/or multiple generations. Meaningful timescales can only be obtained by modelling a significant number of crystals for each population.

## Resolving elemental diffusion stratigraphy

It is well-known that igneous rocks contain a complex crystal cargo which preserve information about a variety of processes occurred over different lengths of time and in different portions of the plumbing system (e.g., Cooper, 2017; Sparks et al., 2019). The simple case of crystals presenting only compositionally zoned rims (Fig. 1a, b) is the most straightforward to resolve and interpret. In these cases, the obtained timescales indicate the time elapsed from the formation of the rim until the eruption. Therefore, it constrains the time spent in the last magmatic environment before eruption, which can be either more mafic or more evolved than the previous magmatic environment (where the core formed). In the specific example of Stromboli, the mafic rim in the clinopyroxene gives a timescale of around four months from the injection of the mafic magma until the eruption (Fig. 1a), suggesting a rapid response of the plumbing system to new injections of mafic magmas, which can trigger the eruption over a short timescale. On the contrary, the longer timescales (~ four years) modelled for the mafic core – evolved rim interface of the orthopyroxene from Popocatépetl (Fig. 1b) suggests a very different dynamics and origin of the crystal. Texture, composition and modelled timescales show that the crystal was remobilized from a mafic to a more evolved magmatic environment, where it spent several years before being erupted. In this case, there is no record of a mafic injection triggering the eruption, and instead gas percolation (Degruyter et al., 2019) and/or second boiling (Cassidy et al., 2018) might have caused the eruption. Alternatively, the mafic injection triggering the eruption was not seen by this particular crystal which might have been stored in a different part of the plumbing system. Clearly, a more in-depth study of the crystal cargo populations is necessary to provide adequate context for a firmer answer.

Relatively simply zoned minerals (Fig. 1c, d) can provide constraints on the timescales spent in different magmatic environments alongside the diffusive storage time and the efficiency of magma dynamics. The NIDIS model (Petrone et al., 2016) facilitates the calculation of a total diffusion residence time ($\Delta t$) defined as the time from the (first) injection of the mafic magma to the eruption. Therefore, it does not correspond to the absolute age or the absolute storage time of the crystal, because the formation of the core cannot be accounted for, but it is tracking the timescale of magma injection, storage and eruption. The diffusion residence time ($\Delta t$) is the sum of two partial timescales: the time spent in the last magmatic environment before the eruption ($\Delta t_2$ or external timescales) corresponding to the diffusion time of the compositional band – rim boundary (in the case of Fig. 1c at the lower T of the more evolved magma); and the time spent in contact with the high-T magma ($\Delta t_1$ or internal core – compositional band boundary) calculated by the relaxation of the core-band diffusion profile after taking into account the external timescale $\Delta t_2$ (for details see Petrone et al., 2016; 2018). The external partial timescale (i.e., band – rim $\Delta t_2$) constrains the final assemblage of the

eruption as in the previous simpler cases (Fig. 1a, b), whereas the internal timescale (i.e., core – band $\Delta t_1$) gives indication on the timescales of crystal transfer from one magmatic environment to the other and/or the efficiency of magma homogenisation process. The most important aspect is that when the two partial timescales are compared together they provide important indication of the storage time in different magmatic environments and therefore on the dynamics of the magmatic system. The examples presented are clinopyroxenes from Stromboli (Fig. 1c) and Popocatépetl (Fig. 1d), which suggest very different magma dynamics. The Stromboli clinopyroxene gives a short residence time (1.8±1 yrs) and, as suggested by Petrone et al. (2018), indicates an efficient magma homogenisation regime, with the internal timescale ($\Delta t_1$) significantly shorter than external ($\Delta t_2$) (0.01 yrs *vs* 1.8 yrs, respectively). On the contrary, the clinopyroxene from Popocatépetl, not only shows a much longer total residence time (267±102 yrs), but it also has a $\Delta t_1$ (174±96 yrs) which is significantly longer than $\Delta t_2$ (93±34 yrs). Following a reasoning similar to Petrone et al. (2018), and considering that whole rock geochemistry indicates that Popocatépetl is characterized by magma hybridization in a long-lived and stable extensive plumbing system (Mangler et al., 2019), we argue that this crystal records melt transport and prolonged storage in multiple magmatic environments, in the order of hundreds of years. In this case, the crystal stratigraphy traces its prolonged path through a complex plumbing system, with no apparent link between magma mafic injections events and eruptions. Similarly, a Popocatépetl orthopyroxene (Fig. 2a) records a magma transfer event resulting in prolonged storage in an evolved magmatic environment ($\Delta t_1$ = 84±42 yrs), however a subsequent mafic injection event rapidly mobilized and erupted the crystal ($\Delta t_2$ = 51±22 days). While these isolated examples from Popocatépetl can clearly not characterize the full extent of magma dynamics of the volcanic system, they show how elemental diffusion chronostratigraphy can help understand the complexity of magmatic plumbing systems and the heterogeneous nature of magmatic reservoirs. Furthermore, it highlights the importance of modelling a large number of crystals from different populations to reveal the full extent of magma dynamics.

Another example is offered by a Stromboli clinopyroxene (Fig. 2b) with a low-Mg# core surrounded by three high-Mg# bands alternating with low-Mg# bands. The timescales calculated with the NIDIS model indicates a total residence time of around 10 years from the first mafic injection until the eruption, with about 5 years spent in each of the two older low-Mg# magma environments. This has been interpreted by Petrone et al. (2018) as indication of multiple injections of the high-Mg# magma in the low-Mg# magma accompanied by short storage, followed by the last mafic injection which triggered the eruption. In fact, in some cases, not only the mafic triggering event can be resolved, but also the on-going hybridization processes (Petrone et al, 2018) up until the eruption, as evident from the stepped right-hand profile in Figure 2c, which having a less steep slope than the internal core-band boundary, cannot be produced by diffusion process. Finally, the timescales of crystal mush remobilization can be retrieved by the elemental diffusion stratigraphy alongside further episodes of

magma injections (Fig. 2d). In this Stromboli clinopyroxene a patchy core surrounded by multiple layers of different compositions, has been interpreted by Petrone et al. (2018) as an antecryst remobilized from the crystal mush by the mafic melt recorded by the high-Mg# layer immediately surrounding it. The crystal has been then delivered in a low-Mg# melt environment where it recorded the arrival of another input of more mafic magma and was stored for about 2 years before moving to the final low-Mg# environment for some 12 years before eruption.

**Uncertainties**

The examples presented above show that elemental diffusion chronostratigraphy, resolved in this case with the non-isothermal diffusion modelling NIDIS, is a powerful tool to reconstruct pre-eruptive histories of single crystals, and – given a sufficiently large sample set – to constrain timescales of magmatic processes in a given plumbing system, such as: magma mixing, crystal transfer and storage, mush remobilization, eruption triggering and ascent to the surface. However, when it comes to interpreting geospeedometry results, it is important to consider the uncertainties related to the modelled timescales, which are fundamentally controlled by the uncertainty related to the diffusion coefficient $D$ and temperature.

The temperature at which diffusion occurs has exponential influence on the diffusivity (eq. 1), and thus uncertainties in the temperature strongly affect the calculated timescales. Commonly used geothermometers (see Putirka et al., 2008 for a review) provide uncertainties in magmatic temperatures in the order of 10 – 50 °C, which result in uncertainties of up to 60 rel. % in modelled timescales (Figs. 1 & 2). However, in cases where the error on the estimated temperature can be drastically reduced ( ± 6 °C; Scarlato et al, this issue), the corresponding error on the estimated timescales is reduced to 20% (Petrone et al., 2016; Scarlato et al., this issue). Therefore, it is extremely important to minimise uncertainties on magmatic temperatures as much as reasonably possible. This requires detailed knowledge of the magmatic system in question and specific calibration of geothermometers, as that recently calibrated for the shoshonitic composition of the present-day activity at Stromboli (Scarlato et al., this issue). Even so, gradual and/or minor temperature fluctuations in the magmatic system may not be resolvable, and therefore uncertainties on temperatures to an extent represent the natural variability of a magmatic system.

In addition to the temperature at which diffusion occurs, $D$s depend on various other physico-chemical variables such as pressure, $X_{mineral}$, $f_{O_2}$ and $f_{H_2O}$ of the host magma (Costa et al., 2008, and references therein). Furthermore, diffusion rates depend on the crystallographic direction, the concentration of the element in question, the diffusion type (e.g., tracer/self vs. chemical diffusion), and the diffusion mechanism (Chakraborty, 1997; Dohmen, Ter Heege, Becker, & Chakraborty, 2016). Some expressions of $D$ allow for variations in other parameters such as composition and $f_{O_2}$

(e.g., Dohmen et al., 2016), but most other variables are commonly accounted for as constant bulk values included in the pre-exponential factor $D_0$ (e.g., Costa & Chakraborty, 2008). Thus, in addition to T, the accuracy and precision of timescales derived from diffusion modelling crucially depends on the accuracy, robustness and applicability of the pre-exponential factor $D_0$ and the activation energy $E$. These factors are commonly derived from experiments, and many diffusion modelling studies assume experimentally obtained $D_0$ and $E$ values to be accurate and precise values. However, as we will show for the example of published $D_{Fe-Mg}$ in orthopyroxene, the uncertainties associated with the experimental determination of *D*s are significant and can affect both their precision and accuracy.

Reliable $D_{Fe-Mg}$ in orthopyroxene have proven difficult to obtain experimentally due to the slow diffusivities involved. Therefore, Fe–Mg diffusion rates in orthopyroxene were initially constrained relative to coexisting garnet in granulite facies rocks (Pattison & Bégin, 1994) and mantle xenoliths (Smith & Barron, 1991), and subsequently also relative to coexisting olivine (Klügel, 2001). The first independent $D_{Fe-Mg}$ in orthopyroxene was developed by Ganguly and Tazzoli (1994) based on experimental data on Fe–Mg fractionation between crystallographic sites (Anovitz et al., 1988; i.e., order-disorder rates; Besancon, 1981; Molin et al., 1991) and crystallographic constraints. Ganguly and Tazzoli (1994) stated that the standard error in *D*s calculated using their expression is 'approximately one order of magnitude', which, if considered in the modelling of timescales, yields greater uncertainties than those introduced by temperature constraints. Ganguly and Tazzoli (1994) identify the dependence of $D_{Fe-Mg}^{opx}$ on the crystallographic direction and oxygen fugacity, however these factors are not accounted for in their expression, and the given standard error is derived from the scatter in experimental data only. Furthermore, their $D_{Fe-Mg}^{opx}$ is based on experiments conducted at $T \approx 500 - 800°C$, $X_{Fe} = 0.1 - 0.5$ and $f_{O_2}$ around the IW buffer, which is not representative for many active volcanic systems.

To overcome the theoretical framework required to calculate *D*s, Schwandt et al. (1998) directly measured Mg self-diffusion coefficients along the three crystallographic axes in three natural crystals with $En_{88}Fs_{12}$ at four temperatures from 750 – 900°C at the IW buffer. Linear least squares fitting of the results yielded Arrhenius relationships (Eq. 1) for the three crystallographic axes of orthopyroxene, giving the first direct constraints on $E$ and $D_0$ along the *a*-, *b*- and *c*-axis in orthopyroxene. Based on their activation energies $E^c < E^b < E^a$, Schwandt et al. (1998) confirmed the diffusion anisotropy ${D_0}^c > {D_0}^b > {D_0}^a$ suggested by Ganguly and Tazzoli (1994). However, large scatter within the dataset resulted in large uncertainties in $E$ and $D_0$ (up to ±70% rel.), to an extent that the respective values for different crystallographic axis are equal within error. This is most apparent for the pre-exponential factors $D_0$, which become increasingly dominant as the temperature rises and the activation energy exerts less control on $D$ (Eq. 1). The pre-exponential factors determined by Schwandt et al. (1998) are highest along the *a*-axis and lowest along the *c*-axis, with ${D_0}^a > {D_0}^b >$

$D_0{}^c$. Using these values to extrapolate $D_{Fe-Mg}$ to magmatic temperatures found at arc volcanoes such as Popocatépetl (~950 – 1100°C) result in the paradoxical situation of $D^a_{Fe-Mg}$ being the fastest, and $D^c_{Fe-Mg}$ the slowest diffusion coefficient (Fig. 3). However, textural evidence unequivocally confirms that diffusion is fastest along the *c*-axis and slowest along the *a*-axis (e.g., Fig. 2a, where diffusive replacement is most advanced along the *c*-axis). The scatter in experimental data thus results in the imprecise and inaccurate determination of $E$ and $D_0$, which becomes apparent upon extrapolation to magmatic conditions relevant to many volcanoes worldwide. Moreover, Schwandt's $D$s are self-diffusion coefficients that do not inherently consider chemical gradients, which puts into question their suitability for modelling of zoned crystals.

The pioneering works of Ganguly and Tazzoli (1994) and Schwandt et al. (1998) represent cornerstones of diffusion modelling in igneous systems, and they facilitated numerous studies yielding fundamental new insights into the dynamics of magmatic processes. However, uncertainties related to experimental data, crystallographic direction, oxygen fugacity, and extrapolation to actual magmatic conditions are commonly overlooked. We point out the importance of considering such uncertainties when interpreting diffusion modelling results.

New experimental data published by Dohmen et al. (2016) provide the first expression of $D_{Fe-Mg}$ in orthopyroxene derived from Fe–Mg interdiffusion under magmatic conditions relevant for many volcanic systems in different tectonic settings. Diffusion in two natural crystals with $En_{98}Fs_1$ and $En_{91}Fs_9$ was measured at $T = 870 - 1100°C$ and $f_{O_2} = 10^{-11} - 10^{-7}$, and Dohmen et al. (2016) show negligible dependency of $D_{Fe-Mg}$ on the orthopyroxene composition if $Fs_{<50}$. This $D_{Fe-Mg}$ can thus be applied to orthopyroxene of most magmatic systems without the need for extrapolation, and it includes a parameter to account for the dependence of $D$ on the oxygen fugacity. Due to the larger dataset produced by Dohmen et al. (2016), uncertainties in $E$ and $D_0$ are better constrained than by Schwandt et al. (1998). However, despite significantly improved uncertainties in $E$ (±5 rel.-%) compared to Schwandt et al. (1998; up to 25 rel.-%), uncertainties in $D_{Fe-Mg}$ after Dohmen et al. (2016) introduce a variability of almost two orders of magnitude in modelled timescales.

This shows that, contrary to common belief, uncertainties introduced by temperature estimates are not necessarily the most significant source of uncertainty on timescales derived from diffusion modelling. While it is crucial to use accurate and precise input data for diffusion modelling (i.e., T, X, $f_{O_2}$), the largest – and mostly neglected – source for uncertainties are those in experimentally derived values for $E$ and $D_0$. These uncertainties are intrinsic to the experimental determination of the $D$ used, so producing better experimental constraints on $E$ and $D_0$ is of utmost importance to increase the accuracy and significance of geospeedometry. Combining diffusion timescales from different minerals and elemental systems can be used to reduce inherent uncertainties and cross-validate diffusion timescales (e.g., Chamberlain et al., 2014; Cooper et al., 2017), and geospeedometry results can be integrated with

and cross-checked against timescales derived from other geological techniques such as radiometric dating (Turner and Costa, 2007; Cooper and Kent, 2014). Thus, careful data processing and mindful interpretation of diffusion-derived geological timescales can provide significant and unique insights into magmatic processes, making geospeedometry a powerful geological tool.

**Conclusions: a way forward.**

Elemental diffusion chronostratigraphy of single crystals preserves time-related information of pre-eruptive magmatic processes, which can be used to reconstruct histories and dynamics of magma reservoirs. The temporal information can be unlocked via geospeedometry, and in the last decade many studies have modelled timescales of a range of pre-eruptive processes, from magma mixing to magma ascent rate, magma storage and remobilization in the shallow crust (e.g., Costa et al., 2008; Dohmen et al., 2017; Petrone et al., 2018; Cooper, 2019; Di Stefano et al., 2020). However, in many cases only the timescale of the last compositional boundary has been resolved, limiting our knowledge of pre-eruptive timescales to those directly preceding the eruption. Therefore, information relative to the lifetime of the crystal might be limited, and the time-related histories of magmatic reservoirs might not be easy to reconstruct. A major obstacle to modelling timescales beyond the outermost rim is the need to accurately constrain temperatures at which diffusion occurred. This is particularly critical when more than one compositional boundary is present, pointing to multiple compositional and physical changes during the lifetime of a crystal. Recent models (Cooper & Kent, 2014) have suggested cold storage conditions, where the mush is locked at near-solidus condition, therefore timescales calculated at pre-eruptive magmatic temperature do not reflect storage timescales but only the final mixing and assemblage of magma shortly before eruption.

Here, we argue that hot storage conditions are typical of magmatic systems characterized by open-system conduits in steady-state, where repeated injections of hotter mafic magma determine the continuous presence of eruptible magma at temperature well above the locked crystal mush. Crystals will spend their lifetime at the temperature of the eruptible magma in the corresponding magmatic environment, and under this condition, derived diffusion timescales approximate the storage of the crystal in question, as shown by recent work on Stromboli (Petrone et al., 2018; Di Stefano et al., 2020). In fact, in these systems, hybridization processes are controlled by long-lived end-members with relatively constant composition kept at relatively constant temperature (e.g., Bragagni et al., 2014; Petrone et al., 2018; Di Renzo et al., 2019; Mangler et al., 2019).

Providing a careful and detailed study of the petrology of a given magmatic system, it is possible to fully resolve the elemental diffusion chronostratigraphy, as we have shown using Fe-Mg interdiffusion in pyroxenes from Stromboli and Popocatépetl as examples. The possibility to retrieve meaningful timescales from diffusion stratigraphy is linked to an in-depth knowledge of the

mineralogy and geochemistry of the crystal cargo and the melt involved, accurate estimates of magmatic temperatures for each environment, and good statistic of modelled crystals. Uncertainties introduced by temperature estimates and other input data for diffusion modelling (i.e., $X$, $f_{O2}$) have large effects on the accuracy of modelled timescales and they can be mitigated to a degree by accurate determination of T. Furthermore, intrinsic sources of uncertainties related to experimentally derived values for the activation energy $E$ and the pre-exponential factor $D_0$ need to be considered when evaluating diffusion timescales. Intrinsic uncertainties can be reduced by calculating independent diffusion timescales for different minerals and diffusion systems, and results can be cross-related to and checked against other geologically derived timescales (i.e., radiometric ages, monitoring time series). Further reduction of uncertainties related to experimentally derived diffusion coefficients should be considered a priority in order to advance and improve elemental diffusion modelling data.

Elemental diffusion chronostratigraphy has been reconstructed using the backward approach of the NIDIS model (Petrone et al., 2016; 2018) which deconstructs the complex diffusion profile in single isothermal steps providing crystal diffusive residence time from mafic injection(s) to eruption alongside timescales of storage in different magmatic environments. These timescales, while not equal to absolute crystal ages, provide insights into the time-integrated dynamics of mixing processes, storage, mush mobilization and eruption triggering events during the lifetime of a single crystal. Using examples from Stromboli and Popocatépetl, we have shown that different dynamics of magmatic systems (e.g., short *vs* long storage; mafic injections triggering eruption *vs* absence of correlation between mafic injection and eruption; efficient magma homogenisation and/or crystal transfer to different magmatic environments) can be resolved by geospeedometry applied to the different portions of complex chemically zoned crystals. Elemental diffusion chronostratigraphy is an extremely powerful tool to obtain time-related temporal information on the dynamics and histories of volcanic plumbing systems. Combined with monitoring data and other petrological, geological and geophysical constraints at active volcanoes, they can greatly enhance our capability to inform volcanic hazard assessments.

## Acknowledgments

The authors would like to thank L. Francalanci for the Stromboli samples. In-depth reviews of S. Tommasini and K. Chamberlain greatly improved the manuscript. We are also grateful to S. Mollo and M. Masotta for the careful editorial handling of the manuscript. The work was financially supported by NERC grant NE/M014584 to CMP, and by Royal Society-Newton Fund International Exchanges Grant IE140605 to CMP.

## References

565 Allan, A. S. R., Morgan, D. J., Wilson, C. J. N., & Millet, M.-A. (2013). From mush to eruption in
566 centuries: assembly of the super-sized Oruanui magma body. *Contributions to Mineralogy and*
567 *Petrology*, *166*(1), 143–164, doi:10.1007/s00410-013-0869-2.

568 Anderson, A. T. (1984). Probable relations between plagioclase zoning and magma dynamics, Fuego
569 Volcano, Guatemala. *American Mineralogist*, *69*(7-8), 660-676.

570 Anovitz, L.M., Essene, E.J., & Dunham, W.R. (1988). Order-disorder experiments on
571 orthopyroxenes; implications for the orthopyroxene geospeedometer. *American Mineralogist, 73*,
572 1060-1073.

573 Arana-Salinas, L., Siebe, C., & Macías, J. L. (2010). Dynamics of the ca. 4965yr 14C BP "Ochre Pumice"
574 Plinian eruption of Popocatépetl volcano, México. *Journal of Volcanology and Geothermal*
575 *Research, 192*(3-4), 212-231. doi: 10.1016/j.jvolgeores.2010.02.022.
576
577 Ayres, M., & Vance, D. (1997). A comparative study of diffusion profiles in Himalayan and
578 Dalradian garnets: constraints on diffusion data and the relative duration of the metamorphic
579 events. *Contributions to Mineralogy and Petrology*, *128*(1), 66-80. doi: 10.1007/s004100050294.
580
581 Barboni, M., Boehnke, P., Schmitt, A. K., Harrison, T. M., Shane, P., Bouvier, A. S., & Baumgartner,
582 L. (2016). Warm storage for arc magmas. *Proceedings of the National Academy of Sciences,*
583 *113*(49), 13959-13964. doi: 10.1073/pnas.1616129113.

584 Bertagnini, A., Métrich, N., Francalanci, L., Landi, P., Tommasini, S., & Conticelli, S,. (2008).
585 Volcanology and magma geochemistry of the present-day activity: constraints on the feeding
586 system. *The Stromboli Volcano, An integrated study of the 2002-2003 eruption, AGU*
587 *Geophysical Monographic Series, Washington DC, 182*, 19 – 38. doi: 10.1029/182GM04

588 Besancon, J.R. (1981). Rate of cation disordering in orthopyroxenes. *American Mineralogist, 66*, 965-
589 973.

590 Bragagni, A., Avanzinelli, R., Freymuth, H., & Francalanci, L. (2014). Recycling of crystal mush-
591 derived melts and short magma residence times revealed by U-series disequilibria at Stromboli
592 volcano. *Earth and Planetary Science Letters*, *404*, 206-219. doi:10.1016/j.epsl.2014.07.028.

593 Barboni, M., Boehnke, P., Schmitt, A. K., Harrison, T. M., Shane, P., Bouvier, A. S., & Baumgartner,
594 L. (2016). Warm storage for arc magmas. Proceedings of the National Academy of Sciences,
595 113(49), 13959-13964. doi: 10.1073/pnas.1616129113.

596 Buening, D., & Buseck, P.R. (1973). Fe-Mg lattice diffusion in olivine. *Journal of Geophysical*
597 *Research, 78*, 6852-6862.

598 Burgisser, A., & Bergantz, G. W. (2011). A rapid mechanism to remobilize and homogenize highly
599 crystalline magma bodies. *Nature, 471*(7337), 212, doi: 10.1038/nature09799.

600 Cashman, K. V., & Giordano, G. (2014). Calderas and magma reservoirs. *Journal of Volcanology and*
601 *Geothermal Research*, 288, 28-45, doi: 10.1016/j.jvolgeores.2014.09.007.

602 Cassidy, M., Manga, M., Cashman, K., & Bachmann, O. (2018). Controls on explosive-effusive
603 volcanic eruption styles. *Nature communications, 9*(1), 2839, doi: 10.1038/s41467-018-05293-3.

604 Chakraborty, S., & Ganguly, J. (1991). Compositional zoning and cation diffusion in garnets,
605 Diffusion, Atomic Ordering, and Mass Transport. *Springer*, pp. 120-175.

606 Chakraborty, S. (1997), Rates and mechanisms of Fe-Mg interdiffusion in olivine at 980°–1300° C,
607 *Journal of Geophysical Research: Solid Earth, 102*, 12317-12331. doi: 10.1029/97JB00208

608 Chakraborty, S. (2006). Diffusion modeling as a tool for constraining timescales of evolution of
609 metamorphic rocks. *Mineralogy and Petrology*, *88*(1-2), 7–27. doi:10.1007/s00710-006-0152-6.

610 Chamberlain, K. J., Morgan, D. J., & Wilson, C. J. (2014). Timescales of mixing and mobilisation in
611 the Bishop Tuff magma body: perspectives from diffusion chronometry. *Contributions to*
612 *Mineralogy and Petrology, 168*(1), 1034. doi: 10.1007/s00410-014-1034-2.

613 Cooper, G. F., Morgan, D. J., & Wilson, C. J. (2017. Rapid assembly and rejuvenation of a large
614 silicic magmatic system: Insights from mineral diffusive profiles in the Kidnappers and Rocky
615 Hill deposits, New Zealand. *Earth and Planetary Science Letters, 473*, 1-13. doi:
616 10.1016/j.epsl.2017.05.036.

617 Cooper, K. M. (2019). Time scales and temperatures of crystal storage in magma reservoirs:
618 implications for magma reservoir dynamics. *Philosophical Transactions of the Royal Society A:*
619 *Mathematical, Physical and Engineering Sciences*, *377*(2139), 20180009.
620 doi:10.1098/rsta.2018.0009.

621 Cooper, K. M. (2017). What does a magma reservoir look like? The "crystal's-eye" view. *Elements,*
622 *13*(1), 23-28, doi: 10.2113/gselements.13.1.23

623 Cooper, K. M., & Kent, A. J. R. (2014). Rapid remobilization of magmatic crystals kept in cold
624 storage. *Nature*, *506*(7489), 480–18. doi:10.1038/nature12991.

625 Costa, F., Dohmen, R., & Chakraborty, S. (2008). Time Scales of Magmatic Processes from Modeling
626 the Zoning Patterns of Crystals, *Reviews in Mineralogy and Geochemistry*, *69*(1), 545–594.
627 doi:10.2138/rmg.2008.69.14.

628 Costa, F., S. Chakraborty, & Dohmen, R. (2003). Diffusion coupling between trace and major
629 elements and a model for calculation of magma residence times using plagioclase. *Geochimica et*
630 *Cosmochimica Acta 67*(12), 2189–2200, doi:10.1016/S0016-7037(02)01345-5.

631 Couch, S., Sparks, R.S.J., & Carroll, M.R. (2001). Mineral disequilibrium in lavas explained by
632 convective self-mixing in open magma chambers. *Nature 411*, 1037. doi: 10.1038/35082540

633 Crank, J. (1979) The mathematics of diffusion. *Oxford university press*, 2nd edition, 414 pp.

634 Davidson, J. P., Morgan, D. J., Charlier, B. L. A., Harlou, R., & Hora, J. M. (2007). Microsampling
635 and Isotopic Analysis of Igneous Rocks: Implications for the Study of Magmatic Systems. *Annu.*
636 *Rev. Earth Planet. Sci.*, *35*(1), 273–311. doi:10.1146/annurev.earth.35.031306.140211.

637 Degruyter, W., Parmigiani, A., Huber, C., & Bachmann, O. (2019). How do volatiles escape their
638 shallow magmatic hearth? *Philosophical Transactions of the Royal Society A: Mathematical,*
639 *Physical and Engineering Sciences. 377*(2139), 20180017. doi:10.1098/rsta.2018.0017.

640 Dimanov, A., & Sautter, V. (2000). "Average" interdiffusion of (Fe, Mn)-Mg in natural diopside.
641 *European Journal of Mineralogy, 12*(4), 749-760. doi: 10.1127/0935-1221/2000/0012-0749.

642 Di Renzo, V., Corsaro, R. A., Miraglia, L., Pompilio, M., & Civetta, L. (2019). Long and short-term
643 magma differentiation at Mt. Etna as revealed by Sr-Nd isotopes and geochemical data. *Earth*
644 *Science Reviews*, *190*, 112–130. doi:10.1016/j.earscirev.2018.12.008.

Di Stefano, F., Mollo, S., Ubide, T., Petrone, C.M., Caulfiled, J., Scarlato, P., Nazzari, M., Andronico, D., & Del Bello, E. (2020). Mush cannibalism and disruption recorded by clinopyroxene crystals at Stromboli volcano: new insights from recent 2003-207 activity. *Lithos, 360-361.* doi:10.1016/j.lithos.2020.105440

Dohmen, R., Ter Heege, J. H., Becker, H. W., & Chakraborty, S. (2016). Fe-Mg interdiffusion in orthopyroxene. *American Mineralogist, 101*(10), 2210-2221. doi: 10.2138/am-2016-5815.

Dohmen, R., Faak, K., & Blundy, J. D. (2017). Chronometry and Speedometry of Magmatic Processes using Chemical Diffusion in Olivine, Plagioclase and Pyroxenes. *Reviews in Mineralogy and Geochemistry*, *83*(1), 535–575., doi:10.2138/rmg.2017.83.16.

Druitt, T. H., Costa, F., Deloule, E., Dungan, M., & Scaillet, B. (2012). Decadal to monthly timescales of magma transfer and reservoir growth at a caldera volcano. *Nature*, doi:10.1038/nature10706.

Francalanci, L., Tommasini, S., Conticelli, S., & Davies, G. R. (1999). Sr isotope evidence for short magma residence time for the 20th century activity at Stromboli volcano, Italy. *Earth and Planetary Science Letters*, *167*(1-2), 61-69. doi: 10.1016/S0012-821X(99)00013-8.

Ganguly, J., & Tazzoli, V. (1994). Fe2+-Mg interdiffusion in orthopyroxene: Retrieval from the data on intracrystalline exchange reaction. *American Mineralogist, 79*(9-10), 930-937.

Ganguly, J., Chakraborty, S., Sharp, T. G., & Rumble, D. (1996). Constraint on the time scale of biotite-grade metamorphism during Acadian Orogeny from a natural garnet-garnet diffusion couple. *American Mineralogist*, *81*(9-10), 1208-1216. doi: 10.2138/am-1996-9-1019.

Giacomoni, P. P., Ferlito, C., Coltorti, M., Bonadiman, C., & Lanzafame, G. (2014). Plagioclase as archive of magma ascent dynamics on "open conduit" volcanoes: the 2001–2006 eruptive period at Mt. Etna. *Earth-science reviews, 138*, 371-393. doi: 10.1016/j.earscirev.2014.06.009.

Gómez-Vazquez, A., De la Cruz-Reyna, S., & Mendoza-Rosas, A. T. (2016). The ongoing dome emplacement and destruction cyclic process at Popocatépetl volcano, Central Mexico. *Bulletin of Volcanology, 78*(9), 58. doi: 10.1007/s00445-016-1054-z.

Hawkesworth, C. J., Blake, S., Evans, P., Hughes, R., Macdonald, R., Thomas, L. E., & Turner, S. P. (2000), Time scales of crystal fractionation in magma chambers - Integrating physical, isotopic and geochemical perspectives, *Journal of Petrology*, *41*(7), 991–1006, doi:10.3749/canmin.50.4.1095.

Fabbro, G. N., Druitt, T. H., & Scaillet, S. (2013). Evolution of the crustal magma plumbing system during the build-up to the 22-ka caldera-forming eruption of Santorini (Greece). *Bulletin of Volcanology*, *75*(12), 767. doi: 10.1007/s00445-013-0767-5.

Kahl, M., Chakraborty, S., Costa, F., & Pompilio M. (2011). Dynamic plumbing system beneath volcanoes revealed by kinetic modeling, and the connection to monitoring data: An example from Mt. Etna. *Earth and Planetary Science Letters*, *308*(1-2), 11–22. doi:10.1016/j.epsl.2011.05.008.

Kahl, M., Chakraborty, S., Costa, F., Pompilio, M., Liuzzo, M., & Viccaro, M. (2013). Compositionally zoned crystals and real-time degassing data reveal changes in magma transfer dynamics during the 2006 summit eruptive episodes of Mt. Etna. *Bulletin of Volcanology, 75*(2), 692. doi:10.1007/s00445-013-0692-7.

689 Kent, A. J., Darr, C., Koleszar, A. M., Salisbury, M. J., & Cooper, K. M. (2010). Preferential eruption
690 of andesitic magmas through recharge filtering. *Nature Geoscience*, *3*(9), 631. *3*(9), 631–636,
691 doi:10.1038/ngeo924.

692 Kilgour, G., Blundy, J., Cashman, K., & Mader, H. M. (2013). Small volume andesite magmas and
693 melt–mush interactions at Ruapehu, New Zealand: evidence from melt inclusions. *Contributions*
694 *to Mineralogy and Petrology*, *166*(2), 371-392. doi:10.1007/s00410-013-0880-7.

695 Klügel, A. (2001). Prolonged reactions between harzburgite xenoliths and silica-undersaturated melt:
696 implications for dissolution and Fe-Mg interdiffusion rates of orthopyroxene. *Contributions to*
697 *Mineralogy and Petrology*, 141, 1-14. doi: 10.1007/s004100000222.

698 Krimer, D., & Costa, F. (2017). Evaluation of the effects of 3d diffusion, crystal geometry, and initial
699 conditions on retrieved time-scales from Fe–Mg zoning in natural oriented orthopyroxene
700 crystals. *Geochimica et Cosmochimica Acta 196*, 271-288, doi: 10.1016/j.gca.2016.09.037.

701 Mangler, M.F. (2018), *Evolution and dynamics of the plumbing system of Popocatépetl volcano,*
702 *Mexico* (Doctoral Dissertation), Imperial College London.

703 Mangler, M.F., Prytulak, J., Gisbert, G., Delgado-Granados, H., and Petrone, C.M. (2019),
704 Interplinian effusive activity at Popocatépetl volcano, Mexico: New insights into evolution and
705 dynamics of the plumbing system, *Volcanica 2*(1), 45 – 72, doi: 10.30909/vol.02.01.4572.

706 Mangler, M. F., Petrone, C. M., Hill, S., Delgado-Granados, H., & Prytulak, J. (2020). A pyroxenic
707 view on magma hybridization and crystallization at Popocatépet Volcano, Mexico. *Frontiers in*
708 *Earth Science, 8*, 362. doi: 10.3389/feart.2020.00362

709 Molin, G., Saxena, S., & Brizi, E. (1991), Iron-magnesium order-disorder in an orthopyroxene crystal
710 from the Johnstown meteorite, *Earth and Planetary Science Letters, 105,* 260-265, doi:
711 10.1016/0012-821X(91)90135-5.

712 Morgan, D. J., Blake, S., Rogers, N. W., De Vivo, B., Rolandi, G., & Davidson, J. P. (2006). Magma
713 chamber recharge at Vesuvius in the century prior to the eruption of AD 79. *Geology*, *34*(10),
714 845-848. doi:10.1130/G22604.1.

715 Morgan, D. J., Blake, S., Rogers, N. W., De Vivo, B., Rolandi, G., Macdonald, R., & Hawkesworth,
716 C. J. (2004). Time scales of crystal residence and magma chamber volume from modelling of
717 diffusion profiles in phenocrysts: Vesuvius 1944. *Earth and Planetary Science Letters*, *222*(3-4),
718 933–946. doi:10.1016/j.epsl.2004.03.030.

719 Mueller, T., Watson, E. B., & Harrison, T. M. (2010), Applications of Diffusion Data to High-
720 Temperature Earth Systems, *Reviews in Mineralogy and Geochemistry*, *72*(1), 997–1038,
721 doi:10.2138/rmg.2010.72.23.

722 Ni, H., Keppler, H., Walte, N., Schiavi, F., Chen, Y., Masotta, M., & Li, Z. (2014). In situ observation
723 of crystal growth in a basalt melt and thedevelopment of crystal size distribution in igneous
724 rocks., *Contributions to Mineralogy and Petrology, 167* (1003). doi:10.1007/s00410-014-1003-9.

725 O'Brien, P. J., & Vrána, S. (1995). Eclogites with a short-lived granulite facies overprint in the
726 Moldanubian Zone, Czech Republic: petrology, geochemistry and diffusion modelling of garnet
727 zoning. *Geologische Rundschau*, *84*(3), 473-488. doi: 10.1007/BF00284515
728
729 Pattison, D., & Bégin, N. (1994). Zoning patterns in orthopyroxene and garnet in granulites:
730 implications for geothermometry. *Journal of Metamorphic Geology. 12*, 387-410. doi:
731 10.1111/j.1525-1314.1994.tb00031.x.

Petrone, C. M., Braschi E., Francalanci L., Casalini M. and Tommasini S. (2018). Rapid mixing and short storage timescale in the magma dynamics of a steady-state volcano.*Earth and Planetary Science Letters*, *492*, 206–221. doi:10.1016/j.epsl.2018.03.055.

Petrone, C. M., Bugatti G., Braschi E. and Tommasini S. (2016). Pre-eruptive magmatic processes re-timed using a non-isothermal approach to magma chamber dynamics. *Nature Communications*, *7*(1), 12946.doi:10.1038/ncomms12946.

Putirka, K. D. (2008). Thermometers and Barometers for Volcanic Systems. *Reviews in Mineralogy and Geochemistry*, *69*(1), 61–120. doi:10.2138/rmg.2008.69.3.

Rout, S. S., & Wörner, G. (2020). Constraints on the pre-eruptive magmatic history of the Quaternary Laacher See volcano (Germany). *Contributions to Mineralogy and Petrology, 175*(8), 1-22.

Rout, S. S., Schmidt, B. C., & Wörner, G. (2020). Constraints on non-isothermal diffusion modeling: An experimental analysis and error assessment using halogen diffusion in melts. *American Mineralogist, 105*(2), 227-238.

Scarlato, P., Mollo, S., Petrone, C.M., Ubide, T, & Di Stefano, F. (2019). Interpreting magma dynamics through a statistically refined thermometer: implication for clinopyroxene Fe-Mg diffusion modelling and sector zoning at Stromboli. *AGU Monograph on Crustal Magmatic System Evolution: Anatomy, Architecture, and Physico- Chemical Processes (Mollo, S.and Masotta, M., Edts), this issue.*

Schaaf, P., Stimac, J., Siebe, C., & Macias, J. L. (2005). Geochemical evidence for mantle origin and crustal processes in volcanic rocks from Popocatépetl and surrounding monogenetic volcanoes, central Mexico. *Journal of Petrology, 46*(6), 1243-1282. doi: 10.1093/petrology/egi015.

Schwandt, C. S., Cygan, R. T., & Westrich, H. R. (1998). Magnesium self-diffusion in orthoenstatite. *Contributions to Mineralogy and Petrology*, 130(3-4), 390-396. doi: 10.1007/s004100050373.

Shea, T., Lynn, K. J., & Garcia, M. O. (2015). Cracking the olivine zoning code: Distinguishing between crystal growth and diffusion. *Geology, 43*(10), 935-938. doi: 10.1130/G37082.1.

Siebe, C., Salinas, S., Arana-Salinas, L., Macías, J. L., Gardner, J., & Bonasia, R. (2017). The~ 23,500 y 14 C BP White Pumice Plinian eruption and associated debris avalanche and Tochimilco lava flow of Popocatépetl volcano, México. *Journal of Volcanology and Geothermal Research, 333*, 66-95. doi: 10.1016/j.jvolgeores.2017.01.011

Sosa-Ceballos, G., Gardner, J. E., & Lassiter, J. C. (2014). Intermittent mixing processes occurring before Plinian eruptions of Popocatepetl volcano, Mexico: insights from textural–compositional variations in plagioclase and Sr–Nd–Pb isotopes. *Contributions to Mineralogy and Petrology, 167*(2). doi: 10.1007/s00410-014-0966-x.

Smith, D. and Barron, B.R. (1991). Pyroxene-garnet equilibration during cooling in the mantle. *American Mineralogist 7*6, 1950-1963.

Sparks, R.S.J, & Cashman, K.V. (2017). Dynamic magma systems: Implications for forecasting volcanic activity, *Elements, 13*(1), 35 – 40. doi: 10.2113/gselements.13.1.35.

Sparks, R. S. J., Annen, C., Blundy, J. D., Cashman, K. V., Rust, A. C., & Jackson, M. D. (2019). Formation and dynamics of magma reservoirs. *Philosophical Transactions of the Royal Society A*, *377*(2139), 20180019.doi:10.1098/rsta.2018.0019.

Streck, M. J. (2008). Mineral textures and zoning as evidence for open system processes. *Reviews in Mineralogy and Geochemistry*, *69*(1), 595-622. doi: 10.2138/rmg.2008.69.15

Tachibana, S., Tamada, S., Kawasaki, H., Ozawa, K., & Nagahara, H. (2013), Interdiffusion of Mg–Fe in olivine at 1,400–1,600° C and 1 atm total pressure, *Physics and Chemistry of Minerals, 40*(6), 511-519, doi: 10.1007/s00269-013-0588-2.

Turner, S., & Costa, F. (2007). Measuring timescales of magmatic evolution. *Elements, 3*(4), 267-272. doi: 10.2113/gselements.3.4.267.

Zellmer, G. F., Blake, S., Vance, D., Hawkesworth, C., & Turner, S. (1999). Plagioclase residence times at two island arc volcanoes (Kameni Islands, Santorini, and Soufriere, St. Vincent) determined by Sr diffusion systematics. *Contributions to Mineralogy and Petrology*, *136*(4), 345–357, doi:10.1007/s004100050543.

Zhang, Y. (2010). Diffusion in Minerals and Melts: Theoretical Background. *Reviews in Mineralogy and Geochemistry*, *72*(1), 5–59. doi:10.2138/rmg.2010.72.2.

**Figure Captions**

Fig. 1: Back-scattered electron (BSE) images of banded pyroxene phenocrysts from Stromboli (modified from Petrone et al., 2018) and Popocatépetl volcanoes, extracted greyscale profiles, and fits modelled using the MATLAB script createfit (Petrone et al., 2016). The blue box in BSE images represents the area the compositional transect is integrated from, using the MATLAB script greyvalues (Petrone et al., 2016). External timescales (e.g., core – rim or band – rim) represent the time elapsed between rim formation, in the last magmatic environment, and the eruption ($\Delta t_2$, shown in blue). Internal timescales (e.g., core – band) from earlier magmatic environments ($\Delta t_1$) are shown in red and represent the time spent at band temperatures, with the effect of diffusion during subsequent storages in different magmatic environments removed (light blue curve). For crystals with both $\Delta t_1$ and $\Delta t_2$ timescales, the total diffusion residence time ($\Delta t = \Delta t_1 + \Delta t_2$) is given. See Petrone et al. (2016) for a detailed description of the NIDIS model. Mg# and respective equilibrium temperatures are given for each compositional zone (Petrone et al., 2018; Petrone unpublished data). (a) Crystal recording months storage in the last magmatic environment prior eruption. Stromboli clinopyroxene, STR273_CPX20 (modified from Petrone et al., 2018). (b) Crystal showing years between mixing and eruption. Popocatépetl orthopyroxene, POP-37_OPX1. (c) Crystal recording a rapid, high-T mixing process (~4 days) followed by 1.8 years of storage in a lower-T environment. Stromboli clinopyroxene, STR275_CPX16 (modified from Petrone et al., 2018). (d) Crystal showing prolonged storage at high temperatures after mixing, followed by decades at lower temperatures. Popocatépetl clinopyroxene, POP-59Y_OPX36. See text for further explanation. Stromboli pyroxenes are from Petrone et al. (2018).

Fig. 2: Back-scattered electron (BSE) images of banded pyroxene phenocrysts from Stromboli (modified Petrone et al., 2018) and Popocatépetl volcanoes, extracted greyscale profiles, and fits modelled using the MATLAB script createfit (Petrone et al., 2016). The blue box in BSE images represents the area the compositional transect is integrated from, using the MATLAB script greyvalues (Petrone et al., 2016). External timescales (e.g., core – rim or band – rim) represent the time elapsed between rim formation, in the last magmatic environment, and the eruption ($\Delta t_2$, shown in blue). Internal timescales (e.g., core – band) from earlier magmatic environments ($\Delta t_1$) are shown in red and represent the time spent at band temperatures, with the effect of diffusion during subsequent storages in different magmatic environments removed (light blue curve). For crystals with both $\Delta t_1$ and $\Delta t_2$ timescales, the total diffusion residence time ($\Delta t = \Delta t_1 + \Delta t_2$) is given. Figures (b) and (d) show finite reservoir models of bands with two diffusing boundaries. See Petrone et al. (2016) for a detailed conceptual discussion. Mg# and respective equilibrium temperatures are given for each compositional zone (Petrone et al., 2018; Mangler et al., 2018). (a) Crystal recording decadal storage at low temperatures (i.e., mush), followed by rapid remobilisation and eruption within ~50 days. Popocatépetl orthopyroxene, POP-112_PX23. (b) Crystal recording three high-T, mafic injections within ten years prior to eruption. Stromboli clinopyroxene, STR273_CPX108 (modified from Petrone et al., 2018). (c) Crystal recording few years of storage in hotter magma and subsequent syn-eruptive ongoing hybridization in the final magmatic environment. Stromboli clinopyroxene, STR276_CPX113 (modified from Petrone et al., 2018). (d) Crystal recording two mafic injections leading to remobilisation and eruption of the crystal within decades. Stromboli clinopyroxene, STR275_CPX14. See text for further explanation. Stromboli pyroxenes are from Petrone et al. (2018).

Fig. 3: $\log D_{Fe\text{-}Mg}$ along crystallographic axes in orthopyroxene as determined by Schwandt et al. (1998) and Dohmen et al. (2016). Experimental temperature ranges are also given, log Ds were extrapolated beyond the ranges using given $D_0$ and dH. Values for Dohmen's Ds assume an oxygen fugacity of $10^{-9.730}$ Pa (Mangler, 2018). The grey area highlights the temperature range of Popocatépetl magmas for reference.

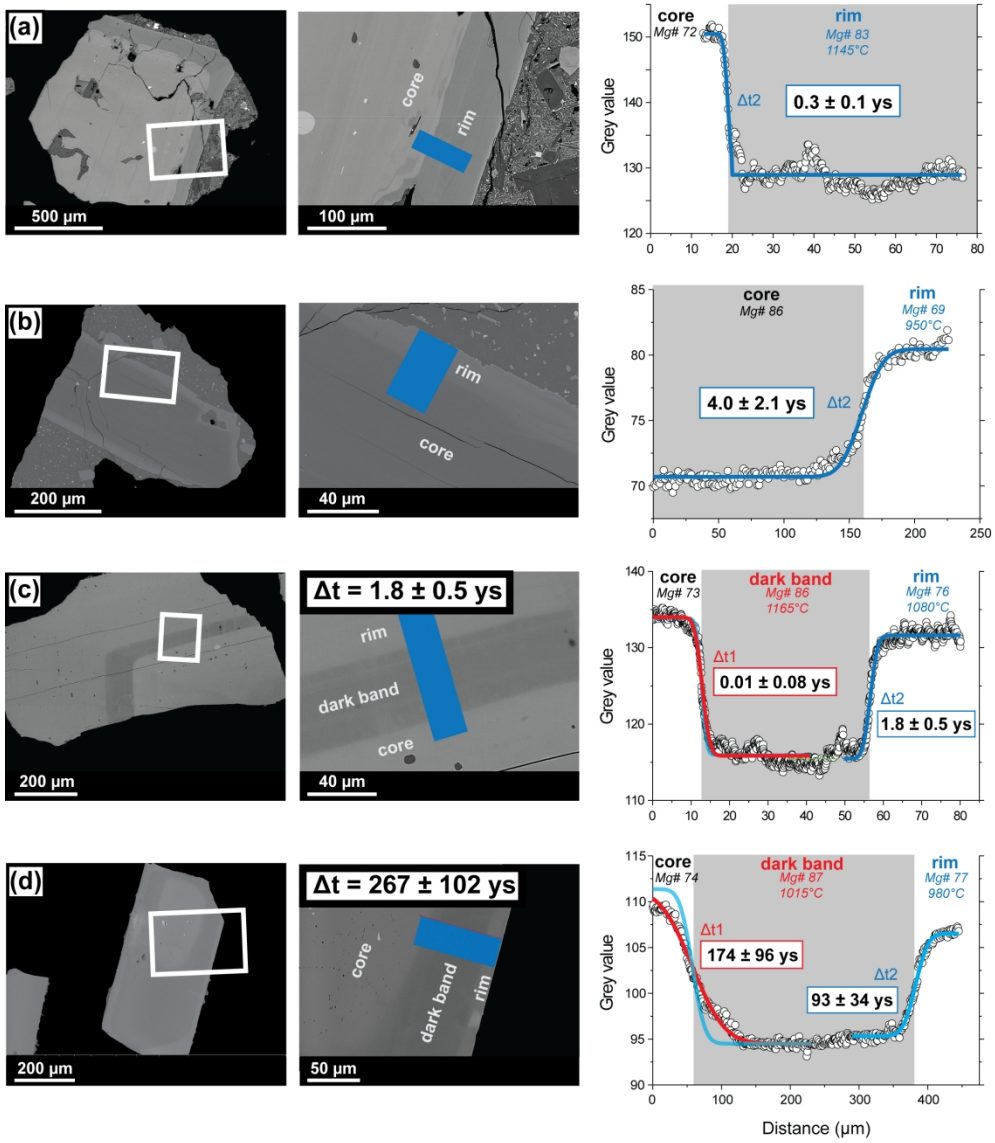


Fig. 1: Back-scattered electron (BSE) images of banded pyroxene phenocrysts from Stromboli (modified from Petrone et al., 2018) and Popocatépetl volcanoes, extracted greyscale profiles, and fits modelled using the MATLAB script createfit (Petrone et al., 2016). The blue box in BSE images represents the area the compositional transect is integrated from, using the MATLAB script greyvalues (Petrone et al., 2016). External timescales (e.g., core – rim or band – rim) represent the time elapsed between rim formation, in the last magmatic environment, and the eruption ($\Delta t_2$, shown in blue). Internal timescales (e.g., core – band) from earlier magmatic environments ($\Delta t_1$) are shown in red and represent the time spent at band temperatures, with the effect of diffusion during subsequent storages in different magmatic environments removed (light blue curve). For crystals with both $\Delta t_1$ and $\Delta t_2$ timescales, the total diffusion residence time ($\Delta t = \Delta t_1 + \Delta t_2$) is given. See Petrone et al. (2016) for a detailed description of the NIDIS model. Mg# and respective equilibrium temperatures are given for each compositional zone (Petrone et al., 2018; Petrone unpublished data). (a) Crystal recording months storage in the last magmatic environment prior eruption. Stromboli clinopyroxene, STR273_CPX20 (modified from Petrone et al., 2018). (b) Crystal showing years between mixing and eruption. Popocatépetl orthopyroxene, POP-37_OPX1. (c) Crystal recording a rapid,

high-T mixing process (~4 days) followed by 1.8 years of storage in a lower-T environment. Stromboli clinopyroxene, STR275_CPX16 (modified from Petrone et al., 2018). (d) Crystal showing prolonged storage at high temperatures after mixing, followed by decades at lower temperatures. Popocatépetl clinopyroxene, POP-59Y_OPX36. See text for further explanation. Stromboli pyroxenes are from Petrone et al. (2018).

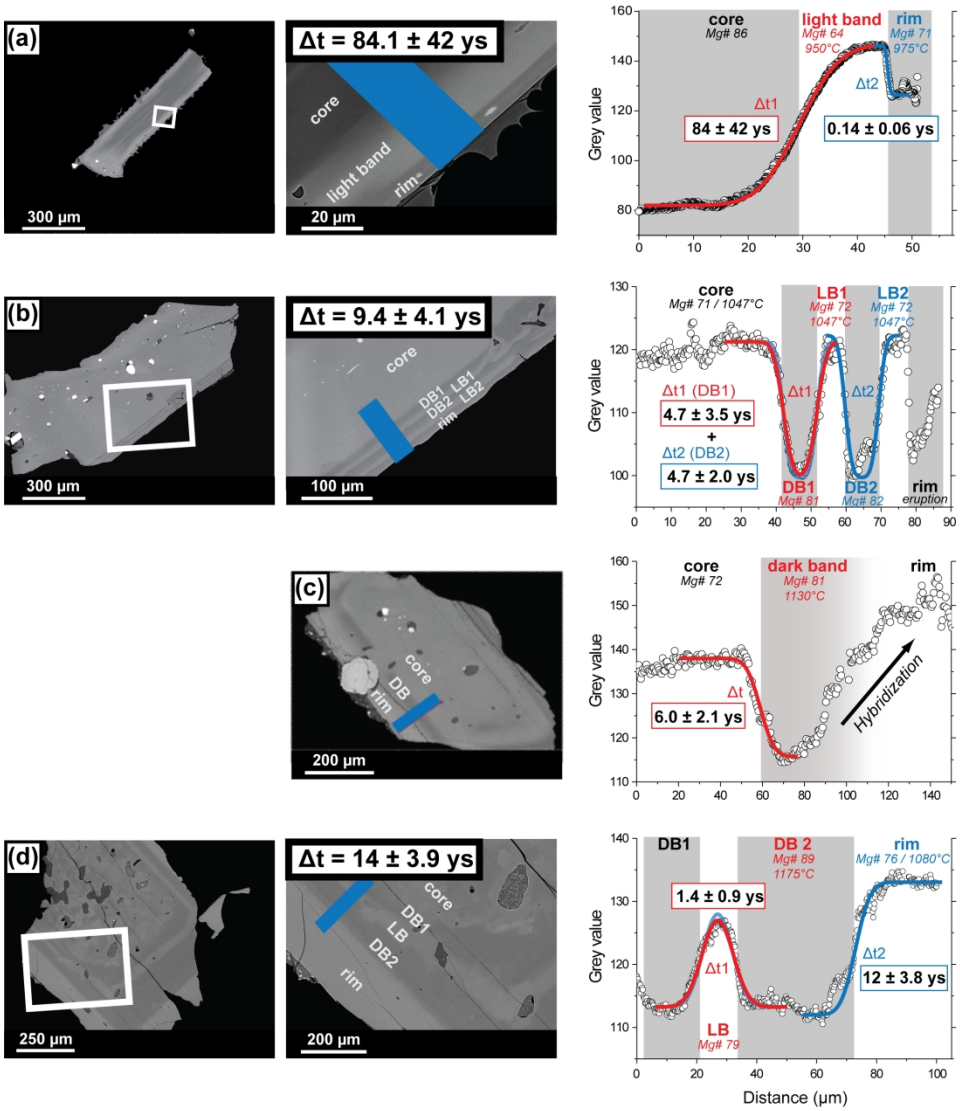


Fig. 2: Back-scattered electron (BSE) images of banded pyroxene phenocrysts from Stromboli (modified Petrone et al., 2018) and Popocatépetl volcanoes, extracted greyscale profiles, and fits modelled using the MATLAB script createfit (Petrone et al., 2016). The blue box in BSE images represents the area the compositional transect is integrated from, using the MATLAB script greyvalues (Petrone et al., 2016). External timescales (e.g., core – rim or band – rim) represent the time elapsed between rim formation, in the last magmatic environment, and the eruption ($\Delta t_2$, shown in blue). Internal timescales (e.g., core – band) from earlier magmatic environments ($\Delta t_1$) are shown in red and represent the time spent at band temperatures, with the effect of diffusion during subsequent storages in different magmatic environments removed (light blue curve). For crystals with both $\Delta t_1$ and $\Delta t_2$ timescales, the total diffusion residence time ($\Delta\square t = \Delta t_1 + \Delta t_2$) is given. Figures (b) and (d) show finite reservoir models of bands with two diffusing boundaries. See Petrone et al. (2016) for a detailed conceptual discussion. Mg# and respective equilibrium temperatures are given for each compositional zone (Petrone et al., 2018; Mangler et al., 2018). (a) Crystal recording decadal storage at low temperatures (i.e., mush), followed by rapid remobilisation and eruption

within ~50 days. Popocatépetl orthopyroxene, POP-112_PX23. (b) Crystal recording three high-T, mafic injections within ten years prior to eruption. Stromboli clinopyroxene, STR273_CPX108 (modified from Petrone et al., 2018). (c) Crystal recording few years of storage in hotter magma and subsequent syn-eruptive ongoing hybridization in the final magmatic environment. Stromboli clinopyroxene, STR276_CPX113 (modified from Petrone et al., 2018). (d) Crystal recording two mafic injections leading to remobilisation and eruption of the crystal within decades. Stromboli clinopyroxene, STR275_CPX14. See text for further explanation. Stromboli pyroxenes are from Petrone et al. (2018).

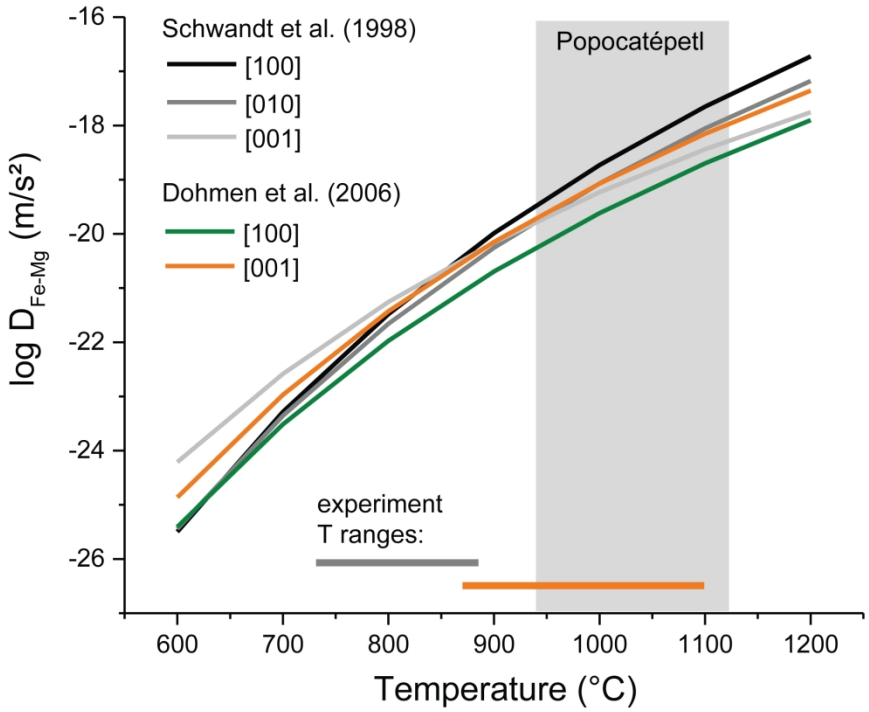


Fig. 3: log$D_{Fe-Mg}$ along crystallographic axes in orthopyroxene as determined by Schwandt et al. (1998) and Dohmen et al. (2016). Experimental temperature ranges are also given, log Ds were extrapolated beyond the ranges using given $D_0$ and dH. Values for Dohmen's Ds assume an oxygen fugacity of $10^{-9.730}$ Pa. The grey area highlights the temperature range of Popocatépetl magmas for reference.